Indian Journal of Pure & Applied Physics
Vol. 64, September 2026, pp. 1053-1062
DOI: 10.56042/ijpap.v64i9.33618

Soliton Propagation in a Homogeneous Electron-positron-ion Plasma having Negatively Charged Dust Grains with Drift and Temperature Effects

Deepak[a] & Hitendra K Malik[b]

[a] Department of Physics, Lajpat Rai College, Ghaziabad 201 005, India

[b] Department of Physics, Plasma Waves and Particle Acceleration Laboratory,
Indian Institute of Technology Delhi, New Delhi 110 016, India

Received: 9th July 2026; accepted: 14th August 2026

The influence of negatively charged dust grains on soliton characteristics is investigated in a homogeneous electron-positron-ion plasma based on the Korteweg-de Vries (KdV) equation obtained using the reductive perturbation technique. The combined effect of dust charge density, ion drift velocity, temperature ratios, and the electron-to-positron density ratio is examined on the soliton characteristics. An increase in the number of negatively charged dust grains significantly modify the medium's nonlinear and dispersive properties, leading to a decrease in soliton amplitude and an increase in its width. When the electron-to-positron density ratio increases, the soliton profile becomes noticeably broader, and its amplitude decreases. This dependence highlights the role of dust grains in altering the soliton dynamics within the electron-positron-ion plasma. Thermal effects and ion drift enhance the soliton propagation and retaining its shape. These findings provide a more comprehensive understanding of nonlinear wave structures in multi-component dusty pair plasmas relevant to both laboratory and astrophysical environments.

Keywords: Soliton propagation, Korteweg-de Vries (KdV) equation, Reductive perturbation technique, Electron-positron-ion plasma, Dusty plasma

1 Introduction

Solitary waves, or solitons, have attracted sustained interest across many branches of physics because of their importance and the variety of systems in which they appear, including fluid dynamics, nonlinear optics, superconductivity, particle theory, and plasma physics[1,2]. In such systems, localized structures emerge when nonlinearity and dispersion balance. In plasmas, ion-acoustic solitons represent a classic example of such structures, and their evolution is governed by the well-known Korteweg-de Vries (KdV) equation[3]. In homogeneous plasmas, this equation provides a reliable description of one-dimensional electrostatic solitons[4,5].

Much of the earlier work focused on electron-ion plasmas, where relatively heavy ions form the inertial component and much lighter electrons are treated as a Boltzmann-distributed, quasi-static background supporting ion-acoustic waves[6,7]. On the other hand, pair plasmas represent a qualitatively distinct regime in which electrons and positrons share equal mass but carry opposite charges, leading to fundamentally different wave dynamics compared to conventional electron-ion plasmas[8,9]. Here, both species participate equally and dynamically in the soliton generation process. Electron-positron plasmas are not only of theoretical interest but are also expected in pulsar magnetospheres, near black holes, quasars, and active galactic nuclei[10-12], and can be produced in extreme astrophysical conditions. Several laboratory experiments have successfully created e-p plasmas[13-14]. It is therefore assumed that pair annihilation is slow compared to the standard plasma time scales in studying the collective behavior of e-p plasmas. Collective modes have been analyzed[15] in nonrelativistic pair plasmas in both magnetized and unmagnetized cases, whereas in another study[16] a multi-fluid approach was employed. Other works[17-19] further examined nonlinear electromagnetic wave dynamics and parametric instabilities in e-p plasmas. Additional investigations included modulated electrostatic wave packets[20], linear wave modes[21], exact electrostatic structures[22], and localized electromagnetic structures in relativistic pair plasmas[23]. In most astrophysical and laboratory environments, including planetary rings, cometary tails, interplanetary space, and purpose-built laboratory devices include charged dust grains[24-26].

Corresponding author: E-mail: hkmalik@physics.iitd.ac.in

Dust grains are significantly more massive than ions and electrons and can be treated as stationary during plasma oscillations. Despite this, dust alters the charge balance and modifies the forces that act to restore charge neutrality[27], impacting the behavior of ion-acoustic and other electrostatic waves. This has been the primary catalyst for the investigation of electron-positron-ion plasmas with negatively charged dust, which are particularly rich in nonlinear wave phenomena. Previous work has been done on the incorporation of positively charged dust in e-p plasmas[27-30], however, most of these analyzes are done with the assumption of zero drift velocities for the plasma constituents, Similarly, solitary and envelope soliton structures were examined in dusty e-p plasmas[31,32], though that treatment did not incorporate ion drift or combined thermal and dust charge effects simultaneously In astrophysical and space environments, drifting electrons and positrons are commonly observed and play an important role in wave excitation, propagation stability, and nonlinear wave-particle interactions[33-35].

Unlike the previous studies, the present work investigates the propagation of solitons in a homogeneous electron-positron-ion plasma containing stationary negatively charged dust grains, where electrons, positrons, and ions are treated as mobile species having initial drifts. The present analysis considers their combined influence within a single framework, enabling us to explore how dust-induced inertia and drift-driven energy transport interact and both affect the nonlinear and dispersive behavior of the system, which have not been explicitly analyzed together in previous investigations of electron-positron-ion plasmas. The analysis is carried out using the reductive perturbation technique (RPT)[36], which expands the normalized fluid and Poisson's equations to obtain the corresponding KdV equation. Expressions for the nonlinear and dispersive coefficients are then derived in terms of key plasma parameters, including temperature ratios, drift velocities, and dust charge. These results are used to examine how these parameters influence the soliton's amplitude, width, and propagation speed. This work aims to better understand the solitary structures in multi-component dusty pair-ion plasmas[37-45]. Furthermore, it extends previous theoretical studies of nonlinear electrostatic solitary waves in multi-component plasmas[46-49] by including the combined effects of ion drift, finite-temperature ratio, and stationary negatively charged dust.

2 Theoretical Model

The plasma considered in the present investigation comprises electrons, positrons, ions, and stationary negatively charged dust grains. Electron-positron plasmas of this type arise naturally in several astrophysical environments[11], active galactic nuclei[12], and the early Universe[10], as well as in controlled laboratory settings[8,13,14]. Following the standard pair-plasma fluid description[15,21], the electrons and positrons have equal mass $(m_e = m_p)$ and equal but opposite charge. The ions, having mass $m_i \gg m_e$ are positively charged and dynamically mobile, unlike the heavier dust grains, that are assumed to remain stationary due to their comparatively greater mass, an assumption widely adopted in the dusty plasma literature[27,28,37]. The plasma species, namely electrons, positrons and ions are considered to have drift velocities. Since the dust grains are stationary, they do not directly provide the wave inertia, instead they modify the equilibrium quasi-neutrality and local composition; thereby influencing the effective restoring force and the nonlinear and dispersive properties of the medium.

2.1 Governing Equations

Using the standard fluid model, the following normalized fluid equations for the positrons electrons and ions are obtained.

The continuity equations are;

$$\frac{\partial n_j}{\partial t} + \frac{\partial}{\partial x}\left(n_j v_j\right) = 0 \qquad \text{... (1a)}$$

The momentum equations are written as;

$$\left(\frac{\partial v_j}{\partial t} + v_j \frac{\partial v_j}{\partial x}\right) = -\frac{q_j}{m_j^i}\frac{\partial \phi}{\partial x} - \frac{\sigma_j}{m_j^i n_j}\frac{\partial n_j}{\partial x} \qquad \text{... (1b)}$$

where $j = p, e, i$, denotes the positron, electron, and ion species, respectively. The charge state is given by $q_j = +1, -1, +1$, for positrons, electrons, and ions, respectively, while $m_j^i = m_j/m_i$ represents the normalized mass ratio of the jth species, where $m = m_e/m_i = m_p/m_i$ and $m_i^i = 1$. Furthermore, $\sigma_j = T_j/T_{eff}$ denotes the normalized temperature ratio of the jth species with the effective temperature T_{eff} (defined later).

Poisson's equation is written as;

$$\frac{(\phi)^2}{x^2} = n_e - n_p - n_i + Z_d n_{d0} \qquad \text{... (1c)}$$

The number densities of electrons, positrons, and ions are n_e, n_p and n_i and the drift velocities of electrons and positrons are represented by v_e, v_p and v_i, respectively. The electrostatic potential is denoted by ϕ. Z_d is the charge number on the dust particles.

Normalization follows the standard approach used in multi-component fluid plasma models[3,37]. Number densities are scaled by the equilibrium ion density, n_{i0}. Velocities are normalized by the effective ion-acoustic speed, $v_s = \sqrt{T_{eff}/m_i}$. The electrostatic potential ϕ is normalized by T_{eff}/e, Space and time are normalized, respectively, by the effective Debye length $\sqrt{\epsilon_0 T_{eff}/n_{i0}e^2}$ and the inverse ion plasma frequency $\sqrt{n_{i0}e^2/\epsilon_0 m_i}$. The effective temperature is defined as $1/T_{eff} = n_{e0}/T_e + n_{p0}/T_p + 1/T_i$.

To investigate solitary wave propagation, the KdV equation is derived by collecting terms at successive orders of the smallness parameter ϵ, which characterizes the strength of the perturbation, in the reductive perturbation expansion[36,37]. For a homogeneous plasma, the perturbation expansions can be written as;

$$f_j = f_{j0} + \epsilon f_{j1} + \epsilon^2 f_{j2} + \dots \qquad \text{...(2a)}$$

where, $j = p, e, i$; $f = v, n$ and the unperturbed ion density is normalized to unity ($n_{i0} = 1$).

The electrostatic potential is expanded as;

$$\phi = \epsilon\phi_1 + \epsilon^2\phi_2 + \dots \qquad \text{... (2b)}$$

The space and time variables are stretched as;

$$\xi = \epsilon^{1/2}(x - \lambda_0 t), \eta = \epsilon^{3/2} t \qquad \text{... (3)}$$

where λ_0 is the wave velocity. As the plasma is homogeneous and nonevolving, the unperturbed quantities, $\partial f_{j0}/\partial\xi = \partial f_{j0}/\partial\eta = 0$, where f_{j0} represents the unperturbed quantities such as v_{e0}, v_{p0} and v_{i0}, n_{e0}, n_{p0} and n_{d0}. Using the RPT, equations are obtained at various orders of ϵ. At the order of $\epsilon^{3/2}$, the continuity equations lead to the following relations;

$$\frac{\partial}{\partial\xi}\left(n_{p0}v_{p1} + n_{p1}v_{p0}\right) - \lambda_0\frac{\partial n_{p1}}{\partial\xi} = 0 \qquad \text{... (4a)}$$

$$\frac{\partial}{\partial\xi}\left(n_{e0}v_{e1} + n_{e1}v_{e0}\right) - \lambda_0\frac{\partial n_{e1}}{\partial\xi} = 0 \qquad \text{... (4b)}$$

$$\frac{\partial}{\partial\xi}\left(v_{i1} + n_{i1}v_{i0}\right) - \lambda_0\frac{\partial n_{i1}}{\partial\xi} = 0 \qquad \text{... (4c)}$$

Correspondingly, the momentum equations at the same order give;

$$-mn_{p0}\lambda_0\frac{\partial v_{p1}}{\partial\xi} + mn_{p0}v_{p0}\frac{\partial v_{p1}}{\partial\xi} + n_{p0}\frac{\partial\phi_1}{\partial\xi} + \sigma_p\frac{\partial n_{p1}}{\partial\xi} = 0 \qquad \text{... (4d)}$$

$$-mn_{e0}\lambda_0\frac{\partial v_{e1}}{\partial\xi} + mn_{e0}v_{e0}\frac{\partial v_{e1}}{\partial\xi} - n_{e0}\frac{\partial\phi_1}{\partial\xi} + \sigma_e\frac{\partial n_{e1}}{\partial\xi} = 0 \qquad \text{... (4e)}$$

$$-\lambda_0\frac{\partial v_{i1}}{\partial\xi} + v_{i0}\frac{\partial v_{i1}}{\partial\xi} + \frac{\partial\phi_1}{\partial\xi} + \sigma_i\frac{\partial n_{i1}}{\partial\xi} = 0 \qquad \text{... (4f)}$$

Poisson's equation at order ϵ provides the following relation between the perturbed densities;

$$n_{p1} + n_{i1} = n_{e1} \qquad \text{... (4g)}$$

Collectively, solving the above equations leads to following relation, from which dispersion relation is obtained.

$$\left\{\frac{n_{p0}}{(mA^2-\sigma_p)} + \frac{n_{e0}}{(mB^2-\sigma_e)} + \frac{1}{(C^2-\sigma_i)}\right\} = 0 \qquad \text{... (5)}$$

It is convenient to introduce $A = \lambda_0 - v_{p0}, B = \lambda_0 - v_{e0}$ and $C = \lambda_0 - v_{i0}$

The phase velocity relation is obtained from Eq. (5) as;

$$\lambda_0 = \frac{(v_{i0}n_0 + mv_{e0}) \pm \sqrt{(m+n_0)(\sigma_p + n_0\sigma_i) - mn_0(v_{e0} - v_{i0})^2}}{(m+n_0)} \qquad \text{... (6)}$$

For the wave propagation, the phase velocity λ_0 should be real and positive. Equation (6) shows that the phase velocity λ_0 is real only if the following inequality is satisfied.

$$|v_{e0} - v_{i0}| \equiv v_0 \leq \sqrt{(m+n_0)(\sigma_p + n_0\sigma_i)/mn_0} \qquad \text{... (6a)}$$

where, $n_0 = (h+1)(1 - Z_d n_{d0})/(h-1)$ and $h = n_{e0}/n_{p0}$ ... (6b)

For the positive and real values of phase velocity of the slow mode (corresponding to negative sign in Eq. (6)) the required condition is obtained as $v_{i0}n_0 + mv_{e0} \geq 0$, and $n_0 v_{i0}^2 + mv_{e0}^2 > \sigma_p + n_0\sigma_i$. Since $m = 1/1836$, the electron contribution is negligible, and to satisfy this condition requires a relatively large ion streaming velocity v_{i0}. However, in the present plasma model, v_{i0} always remains smaller than the electron streaming velocity v_{e0} in view of their larger mass. Consequently, the above conditions cannot be satisfied for the chosen set of plasma parameters.

Therefore, the soliton corresponding to the slow mode does not evolve in the present study.

2.2 Korteweg-de Vries (KdV) Equation and Its Solution

To study the soliton propagation, following the standard RPT procedure, a KdV equation is derived based on various equations obtained at higher orders of ϵ. The relevant equations are given below. At the order of $\epsilon^{5/2}$, the continuity and momentum equations lead to the following set of relations

$$\frac{\partial n_{p1}}{\partial \eta} - \lambda_0 \frac{\partial n_{p2}}{\partial \xi} + \frac{\partial}{\partial \xi}\left(n_{p0}v_{p2} + n_{p1}v_{p1} + n_{p2}v_{p0}\right) = 0 \quad \text{... (7a)}$$

$$\frac{\partial n_{e1}}{\partial \eta} - \lambda_0 \frac{\partial n_{e2}}{\partial \xi} + \frac{\partial}{\partial \xi}\left(n_{e0}v_{e2} + n_{e1}v_{e1} + n_{e2}v_{e0}\right) = 0 \quad \text{... (7b)}$$

$$\frac{\partial n_{i1}}{\partial \eta} - \lambda_0 \frac{\partial n_{i2}}{\partial \xi} + \frac{\partial}{\partial \xi}\left(v_{i2} + n_{i1}v_{i1} + n_{i2}v_{i0}\right) = 0 \quad \text{... (7c)}$$

$$mn_{p0}\frac{\partial v_{p1}}{\partial \eta} - mn_{p0}\lambda_0 \frac{\partial v_{p2}}{\partial \xi} + mn_{p0}v_{p0}\frac{\partial v_{p2}}{\partial \xi} + mn_{p0}v_{p1}\frac{\partial v_{p1}}{\partial \xi} + mn_{p1}v_{p0}\frac{\partial v_{p1}}{\partial \xi} - mn_{p1}\lambda_0\frac{\partial v_{p1}}{\partial \xi} + n_{p0}\frac{\partial \phi_2}{\partial \xi} + n_{p1}\frac{\partial \phi_1}{\partial \xi} + \sigma_p \frac{\partial n_{p2}}{\partial \xi} = 0 \quad \text{... (7d)}$$

$$mn_{e0}\frac{\partial v_{e1}}{\partial \eta} - mn_{e0}\lambda_0 \frac{\partial v_{e2}}{\partial \xi} + mn_{e0}v_{e0}\frac{\partial v_{e2}}{\partial \xi} + mn_{e0}v_{e1}\frac{\partial v_{e1}}{\partial \xi} + mn_{e1}v_{e0}\frac{\partial v_{e1}}{\partial \xi} - mn_{e1}\lambda_0\frac{\partial v_{e1}}{\partial \xi} - n_{e0}\frac{\partial \phi_2}{\partial \xi} - n_{e1}\frac{\partial \phi_1}{\partial \xi} + \sigma_e \frac{\partial n_{e2}}{\partial \xi} = 0 \quad \text{... (7e)}$$

$$\frac{\partial v_{i1}}{\partial \eta} - \lambda_0 \frac{\partial v_{i2}}{\partial \xi} + v_{i0}\frac{\partial v_{i2}}{\partial \xi} + v_{i1}\frac{\partial v_{i1}}{\partial \xi} + n_{i1}v_{i0}\frac{\partial v_{i1}}{\partial \xi} - n_{i1}\lambda_0\frac{\partial v_{i1}}{\partial \xi} + \frac{\partial \phi_2}{\partial \xi} + n_{i1}\frac{\partial \phi_1}{\partial \xi} + \sigma_i \frac{\partial n_{i2}}{\partial \xi} = 0 \quad \text{... (7f)}$$

Similarly, Poisson's equation at order ϵ^2 gives rise to;

$$\frac{\partial^2 \phi}{\partial \xi^2} - n_{e2} + n_{p2} + n_{i2} = 0 \quad \text{... (7g)}$$

Combining the above equations with the linearized Eqs. (4a)–(4g) and systematically eliminating the second-order perturbed quantities, following equation is obtained in terms of the first-order ion density perturbation n_{i1}.

$$(C^2 - \sigma_i)\frac{\partial^3 n_{i1}}{\partial \xi^3} + \left\{\frac{(3C^2-\sigma_i)}{(C^2-\sigma_i)} + \frac{\{3mA^2-\sigma_p\}}{(mA^2-\sigma_p)}K^2 - \frac{\{3mB^2-\sigma_e\}}{(mB^2-\sigma_e)}L^2\right\} n_{i1}\frac{\partial n_{i1}}{\partial \xi} + 2\left\{\frac{C}{(C^2-\sigma_i)} + \frac{mAK}{(mA^2-\sigma_p)} - \frac{mBL}{(mB^2-\sigma_e)}\right\}\frac{\partial n_{i1}}{\partial \eta} + \left\{\frac{n_{p0}}{(mA^2-\sigma_p)} + \frac{n_{e0}}{(mB^2-\sigma_e)} + \frac{1}{(C^2-\sigma_i)}\right\}\frac{\partial \phi_2}{\partial \xi} = 0 \quad \text{... (8)}$$

Parameters K and L are defined as $K = (C^2 - \sigma_i)n_{p0}/(mA^2 - \sigma_p)$ and $L = K + 1$. The coefficient of $\frac{\partial \phi_2}{\partial \xi}$ vanishes with the use of the phase velocity relation (5). This leads to the following KdV equation, ensuring the evolution of soliton correspondingly to the wave excited in the plasma.

$$\frac{\partial n_{i1}}{\partial \eta} + \alpha\, n_{i1}\frac{\partial n_{i1}}{\partial \xi} + \beta \frac{\partial^3 n_{i1}}{\partial \xi^3} = 0 \quad \text{... (9)}$$

where α and β describing the nonlinear and dispersive coefficients[3, 37] are given as;

$$\alpha = \frac{\left\{\frac{(3C^2-\sigma_i)}{(C^2-\sigma_i)} + \frac{\{3mA^2-\sigma_p\}}{(mA^2-\sigma_p)}K^2 - \frac{\{3mB^2-\sigma_e\}}{(mB^2-\sigma_e)}L^2\right\}}{2\left\{\frac{C}{(C^2-\sigma_i)} + \frac{mAK}{(mA^2-\sigma_p)} - \frac{mBL}{(mB^2-\sigma_e)}\right\}}, \beta = \frac{(C^2-\sigma_3)}{2\left\{\frac{C}{(C^2-\sigma_i)} + \frac{mAK}{(mA^2-\sigma_p)} - \frac{mBL}{(mB^2-\sigma_e)}\right\}}.$$

Since the first-order perturbed ion density is related to the first-order perturbed electrostatic potential through;

$$(C^2 - \sigma_i)n_{i1} = \phi_1 \quad \text{... (9a)}$$

The KdV equation can be readily expressed in terms of the first-order perturbed electrostatic potential, ϕ_1, as follows;

$$\frac{\partial \phi_1}{\partial \eta} + \alpha' \phi_1 \frac{\partial \phi_1}{\partial \xi} + \beta' \frac{\partial^3 \phi_1}{\partial \xi^3} = 0 \quad \text{... (10)}$$

where the modified nonlinear and dispersive coefficients are given by;

$\alpha' = \alpha/(C^2 - \sigma_i)$ and $\beta' = \beta$

To get the solution of the KdV Eq. (9), following travelling wave transformation is introduced[2,3];

$$X = \xi - U\eta \quad \text{... (11)}$$

Here, *U* represents the soliton velocity. Actually λ_0 is the phase velocity of the wave in the laboratory frame of reference. This wave is excited in the plasma and under the balance of nonlinearity and dispersion, it takes the form of soliton. The soliton moves with velocity U w.r.t. the wave frame of reference. Substituting transformation (11) into Eq. (9) converts the partial differential equation into the following ordinary differential equation

$$-U\frac{\partial n_{i1}}{\partial X} + \alpha\, n_{i1}\frac{\partial n_{i1}}{\partial X} + \beta \frac{\partial^3 n_{i1}}{\partial X^3} = 0 \quad \text{... (12)}$$

For a localized solitary wave, applying the boundary conditions that n_{i1} and its derivatives vanish as $X \to \pm\infty$, and integrating twice, following soliton solution is obtained;

$$n_{i1}\,(\xi - U\eta) = \frac{3U}{\alpha}\,\mathrm{sech}^2\left[\frac{(\xi-U\eta)}{\sqrt{\frac{4\beta}{U}}}\right] \qquad \text{... (13)}$$

This is also written as;

$$n_{i1}\,(X) = n_{im}\,\mathrm{sech}^2[X/W] \qquad \text{... (14)}$$

The standard sech^2 solution of the KdV equation[1,3] yields a compressive soliton, with peak amplitude $n_{im} = 3U/\alpha$ and spatial width $W = \sqrt{4\beta/U}$. The soliton amplitude scales linearly with U and inversely with the nonlinear coefficient α, while the width decreases as U increases, consistent with the fundamental KdV balance between nonlinearity and dispersion[1,2,5].

Following the same procedure, the solution of Eq. (10) for the first-order electrostatic potential can be obtained in an entirely analogous manner. The solution is given by;

$$\phi_1\,(X) = \phi_m\,\mathrm{sech}^2\left[X/W_\phi\right] \qquad \text{... (15)}$$

where, $\phi_m = 3U/\alpha'$ and, $W_\phi = \sqrt{4\beta'/U}$
Energy E of the soliton[49] is given by

$$E = \int_{-\infty}^{\infty} n_{i1}^2\,(X)dX \qquad \text{... (16)}$$

Substituting Eq. (14) into the above expression gives rise to;

$$E = n_{im}^2 \int_{-\infty}^{\infty} \mathrm{sech}^4[X/W]\,dX = 4n_{im}^2 W/3 \qquad \text{... (17)}$$

3 Results and Discussion

The results presented in this section are based on analytical expressions derived from the KdV framework developed in the preceding sections. The effect of key plasma parameters, namely the dust charge valency (Z_d), dust concentration (n_{d0}), ion drift velocity (v_{i0}), ion-to-electron temperature ratio (T) and electron-to-positron density ratio (h) is investigated systematically on the phase velocity, nonlinear coefficient, soliton amplitude, and soliton width. The chosen parameter ranges are representative of astrophysical and laboratory electron-positron-ion dusty plasmas, including environments such as pulsar magnetospheres and active galactic nuclei[10-12].

Figure 1 shows that the phase velocity decreases steadily as Z_d increases, whereas it increases with increasing ion drift velocity. The decrease of λ_0 with Z_d can be understood from the phase-velocity expression. The dust contributes to the system through terms governing both the effective inertia and the electrostatic restoring force. As Z_d increases, the inertial contribution increases more rapidly than the restoring force, leading to a decrease in λ_0. Physically, negatively charged dust grains form a massive stationary background that restricts the free motion of electrons and positrons. This behavior is consistent with the other finding[37], i.e. a similar monotonic decrease in phase velocity with dust concentration in a moving e-p pair plasma with negatively charged dust, and with the broader class of dusty plasma studies[24,27,28]. The present work extends these observations by incorporating ion drift alongside dust charge effects, revealing that the two parameters exert opposing influences on λ_0. Moving ions supply additional energy and momentum to the propagating wave, enhancing the effective restoring mechanism and raising λ_0[33-35,37]. This is consistent with the general physics of wave-particle interactions in drifting plasmas and has been confirmed in recent studies of multi-component plasma systems[39-42,46]. The present finding adds a new dimension by demonstrating that ion drift can partially compensate for the phase velocity reduction caused by dust, a feature not explicitly discussed in earlier pair-plasma studies[37,38].

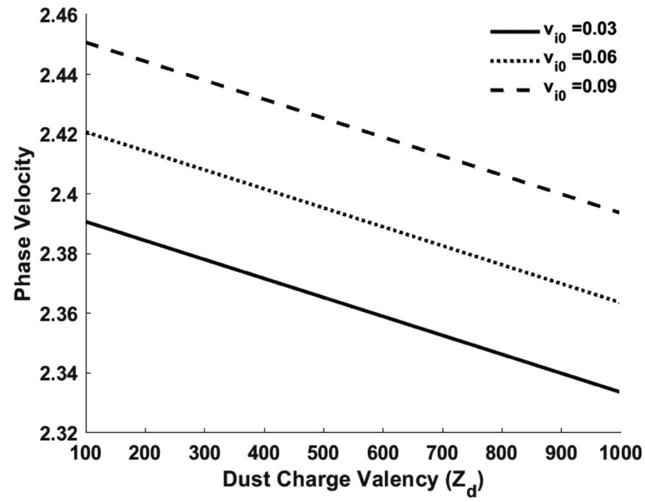

Fig. 1 — Variation of phase velocity with dust charge valency (Z_d) for different ion drift velocities, when $v_{p0} = 0.30$, $v_{e0} = 0.30$, $n_{d0} = 10^{-4}$, h =1.2 and T = 0.1

Figure 2 shows the phase velocity λ_0 varies with the ion-to-electron temperature ratio T for different values of the dust charge density $Z_d n_{d0}$. The temperature dependence of λ_0 enters through the normalized parameters σ_p, σ_e and σ_i in Eq. (6), which

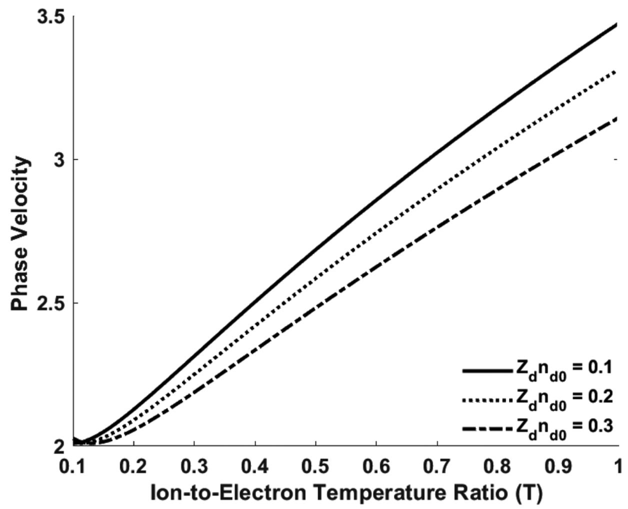

Fig. 2 —Variation of phase velocity with ion-to-electron temperature ratio (T) for different dust charge density $Z_d n_{d0}$, when $v_{p0} = 0.30$, $v_{e0} = 0.30$, $v_{i0} = 0.01$ and $h = 1.2$

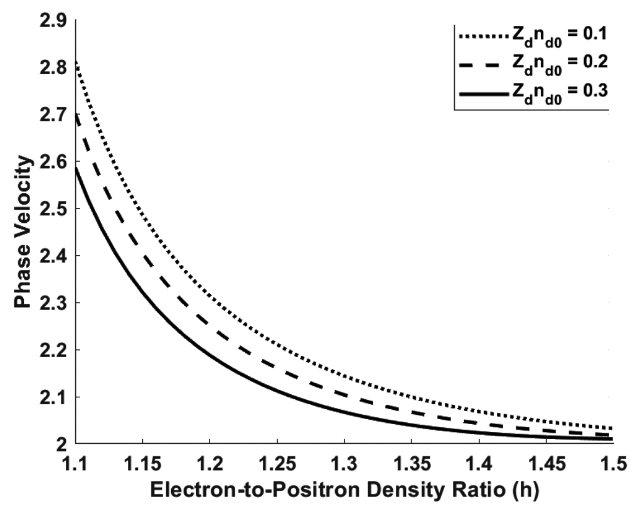

Fig. 3 — Variation of phase velocity with electron-to-positron density ratio (h) for different dust charge density $Z_d n_{d0}$, when $v_{p0} = 0.30$, $v_{e0} = 0.30$, $v_{i0} = 0.01$, and $T = 0.5$
,

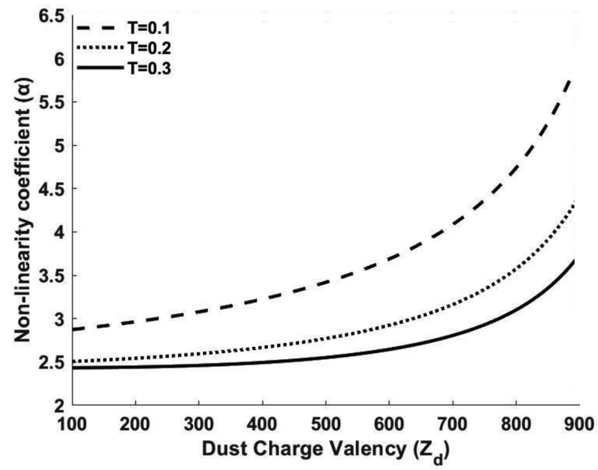

Fig. 4 — Variation of non-linearity coefficient with dust charge valency (Z_d) for different ion-to-electron temperature ratio (T), when $v_{p0} = 0.30$, $v_{e0} = 0.30$, $v_{i0} = 0.01$, $n_{d0} = 10^{-3}$, $U = 1.1$, and $h = 1.2$

represent thermal contributions of the plasma species.

Figure 3 shows the variation of phase velocity λ_0 with the electron-to-positron density ratio h for different values of the dust charge density $Z_d n_{d0}$. As h increases, the relative electron population becomes more dominant, modifying the equilibrium charge balance and leading to stronger electrostatic screening within the plasma[9,10]. This enhanced screening weakens the effective restoring force responsible for wave propagation, thereby reducing λ_0. For any fixed h, increasing $Z_d n_{d0}$ further shifts the curves downward, an effect already well established in Figs. 1 and 2 and attributed to the additional inertia of the negatively charged dust grains. The finding that compositional asymmetry (through h) and dust content independently suppress the phase velocity is in qualitative agreement with recent investigations of electron-positron-ion plasmas[39,43], which show that deviations from symmetric composition substantially alter the medium's dispersion properties. The present study reinforces these findings and extends them to a configuration that also includes ion drift and finite dust charge valency.

Figure 4 shows that the coefficient α increases monotonically with Z_d for all values of T, indicating that the presence of negatively charged dust enhances the nonlinear response of the plasma. Physically, dust grains intensify electrostatic interactions among the plasma species and raise the effective inertia, both of which promote stronger nonlinear steepening. For a fixed Z_d, α decreases with increasing T, since higher ion temperature raises the thermal pressure. These observations are consistent with the results that α increases with dust density in a moving e-p pair plasma[37], as also observed in more recent investigations of multi-component dusty plasmas[40,41,44]. A notable distinction in the present work is the simultaneous inclusion of ion temperature and ion drift, which allows for a more complete characterization of how thermal effects temper dust-driven nonlinearity. Specifically, the present results demonstrate that the influence of T on α is relatively stronger at lower dust levels, becoming progressively subordinate to dust effects as Z_d grows. This hierarchy of competing influences has not been

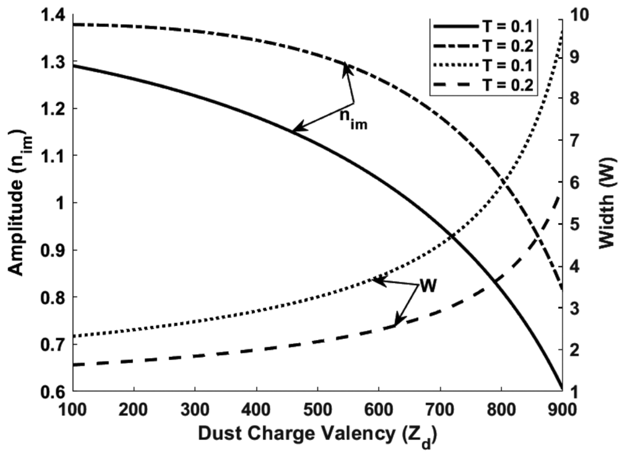

Fig. 5 — Variation of amplitude and width of soliton with dust charge valency (Z_d) for different ion-to-electron temperature ratio (T), when $v_{p0} = 0.30$, $v_{e0} = 0.30$, $v_{i0} = 0.01$, $n_{d0} = 10^{-3}$, $U = 1.1$, and $h = 1.2$

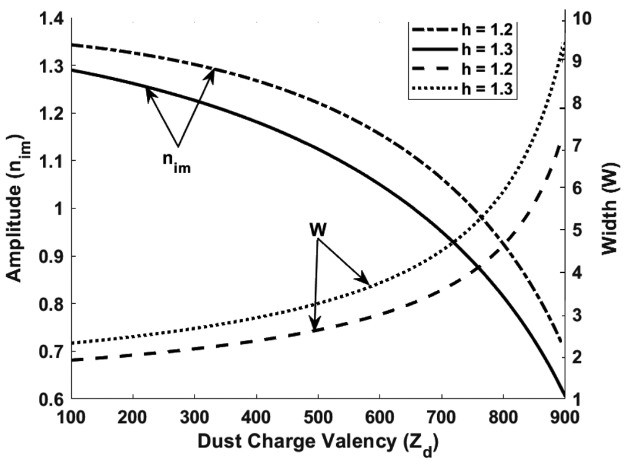

Fig. 6 — Variation of amplitude and width of soliton with dust charge valency (Z_d) for different electron-to-positron density ratio (h), when $v_{p0} = 0.30$, $v_{e0} = 0.30$, $v_{i0} = 0.01$, $n_{d0} = 10^{-3}$, $U = 1.1$, and $T = 0.5$

explicitly identified in previous studies and represents a new physical insight from the present analysis[37,45].

The soliton's amplitude decreases while its width increases when the dust charge valency Z_d is increased (Fig. 5). It means soliton becomes less energetic when the dust particles of larger charge are present in the plasma. This can be understood based on the energy[49] E of the soliton, given by Eq. (17). The soliton energy being proportional to the square of its amplitude causes soliton to be less energetic with Z_d. Moreover, the inverse relationship between amplitude and width is a fundamental characteristic of KdV solitons, reflecting the interplay between nonlinearity and dispersion. In physical terms, dust grains reduce the efficiency of nonlinear steepening while simultaneously enhancing dispersive spreading, so the soliton becomes weaker and more spatially extended. The influence of T is found to yield a larger amplitude because elevated ion temperature reduces α and strengthens the nonlinear character of the wave. This competing behavior, in which temperature enhances amplitude at low dust levels, but dust suppresses it at high dust levels, is a new quantitative result that complements and extends the other findings[41,44].

Figure 6 illustrates that the soliton amplitude and width vary with dust charge valency Z_d for two different electron-to-positron density ratios. Consistent to Fig. 5, the amplitude of the soliton decreases, while its width increases with higher value of Z_d. The effect of h on the soliton structure operates indirectly through its influence on phase velocity, as established in Figure 3. Increasing h reduces the phase velocity, which in turn modifies both α and β through their functional dependence on λ_0. A higher h introduces greater asymmetry between the electron and positron populations, thereby enhancing electrostatic screening and weakening the plasma's nonlinear energy-focusing capacity[9,10]. The result is a soliton with lower amplitude and broader spatial extent. This behavior is consistent with recent theoretical work on asymmetric e-p-i plasmas[42,43], in which compositional imbalance has been identified as a key factor in weakening nonlinear structures. The present results further clarify that the effects of h and Z_d act in the same direction, both suppressing amplitude and broadening the soliton, suggesting that compositional and dusty-medium asymmetries are effectively cooperative mechanisms in degrading soliton coherence.

Figure 7 shows that the soliton amplitude and width vary with the ion-to-electron temperature ratio $T = T_i/T_e$ for different dust charge densities. A clear pattern emerges from the plot with the increasing temperature ratio T that the soliton's amplitude increases while its width decreases. In other words, higher ion temperature leads to taller, more localized (narrower) solitons. This behaviour can be explained as the temperature dependence of the governing coefficients. As T increases, α decreases (Fig. 4), raising the amplitude $3U/\alpha$, while the reduced β narrows the width $\sqrt{4\beta/U}$. Physically, elevated ion temperature intensifies the pressure imbalance in the plasma, strengthens the nonlinear response and

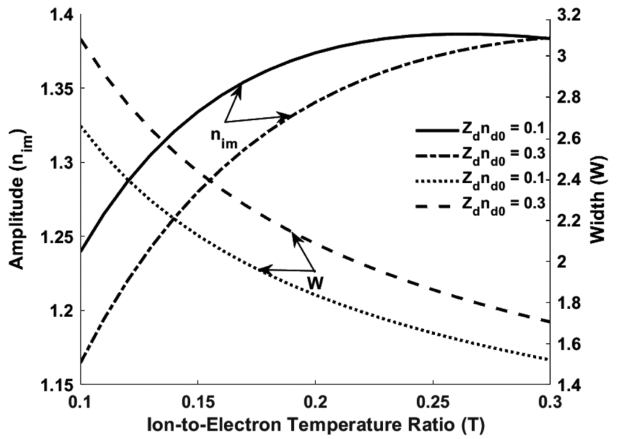

Fig. 7 — Variation of amplitude and width of soliton with ion-to-electron temperature ratio (T) for different dust charge density $Z_d n_{d0}$ when $v_{p0} = 0.30$, $v_{e0} = 0.30$, $v_{i0} = 0.01$, $U = 1.1$, and $h = 1.2$

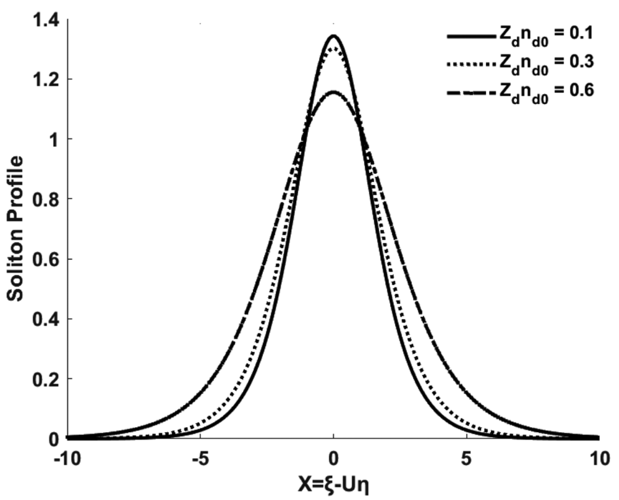

Fig. 8 — Sketch of the soliton profile, showing the effect of dust change density $Z_d n_{d0}$, when $v_{p0} = 0.30$, $v_{e0} = 0.30$, $v_{i0} = 0.01$, $T = 0.1$, $U = 1.1$, and $h = 1.2$

promotes sharper, more energetic solitary structures. This is qualitatively consistent with the other finding[45]. The contribution of the present work lies in demonstrating that this temperature-driven sharpening is modulated by the dust content. For higher $Z_d n_{d0}$, the amplitude is suppressed, and the width remains broader at all values of T. This indicates that dust suppresses the nonlinear effect and enhances dispersion. Another point to note is that the decrease in width with temperature is more pronounced for lower dust levels. This suggests that thermal effects are more effective at sharpening the soliton when the dust density is relatively low. This interplay between temperature-driven nonlinearity and dust-induced dispersion is consistent with other studies on nonlinear wave propagation in dusty plasma systems[41].

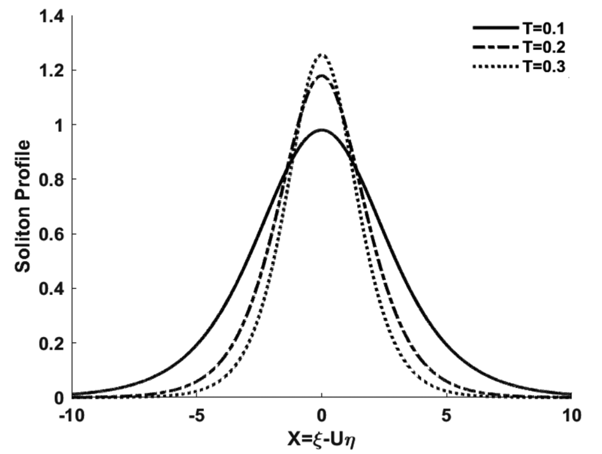

Fig. 9 — Sketch of the soliton profile, showing the effect of the ion-to-electron temperature ratio T, when $v_{p0} = 0.30$, $v_{e0} = 0.30$, $v_{i0} = 0.01$, $Z_d n_{d0} = 0.5$, $U = 1.1$, and $h = 1.2$

Figure 8 shows the comparison of soliton profiles (corresponding to Eq. (14)) for different values of dust change density $Z_d n_{d0}$. The figure clearly shows that the soliton becomes lower in amplitude and broader in width as the dust concentration increases. In other words, higher dust levels lead to weaker and less localized solitary structures. This behaviour can be understood as an increase in dust concentration leads to an increase in both the nonlinear coefficient α and the dispersion coefficient β. As a result, the amplitude decreases while the width increases. Physically, negatively charged dust grains introduce additional inertia and enhance electrostatic shielding, thereby suppressing nonlinear steepening and spreading wave energy over a larger spatial region. The combined effect is a broader, lower-amplitude pulse, as shown in the figure. This behavior is consistent with the profile-level results of other investigators[37,44].

Figure 9 illustrates the effect of the ion-to-electron temperature ratio T on the soliton profile (corresponding to Eq. (14)). As T increases from 0.1 to 0.3, the soliton becomes distinctly taller and narrower, with the peak amplitude rising substantially and the width decreasing. In simple terms, higher ion temperature leads to more localized and energetic solitary structures, whereas lower temperatures produce broader and less pronounced solitons. This behaviour is consistent with the trends observed in Fig. 7 and can be understood through the dependence of amplitude and width on the temperature ratio.

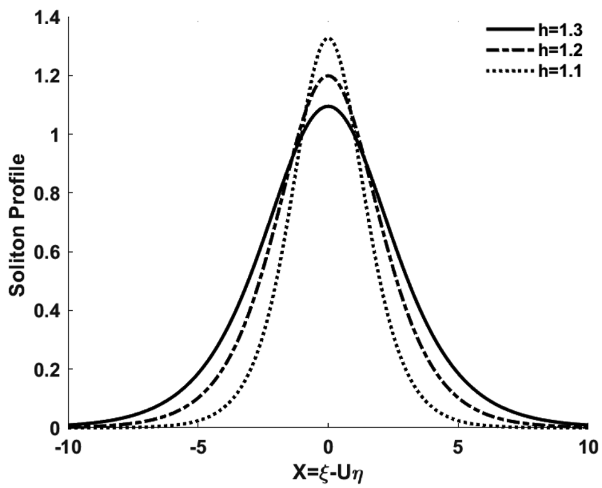

Fig. 10 — Sketch of the soliton profile, showing the effect of electron-to-positron density ratio (h), when $v_{p0} = 0.30$, $v_{e0} = 0.30$, $v_{i0} = 0.01$, $Z_d n_{d0} = 0.5$, $U = 1.1$, and $T = 0.1$

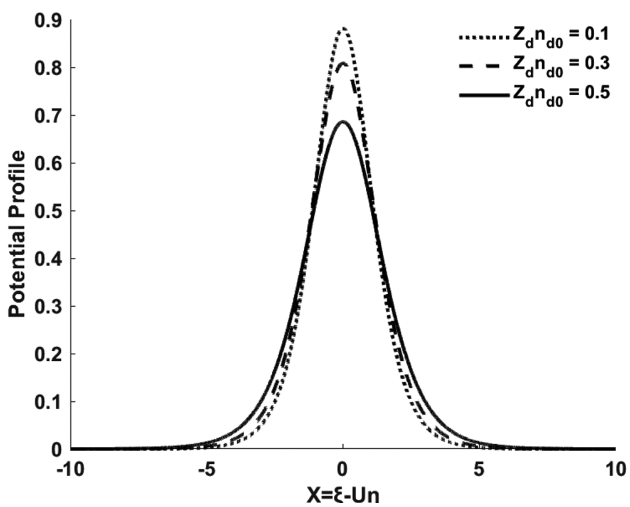

Fig. 11 — Sketch of the first-order electrostatic potential profile, showing the effect of dust change density ($Z_d n_{d0}$), when $v_{p0} = 0.30$, $v_{e0} = 0.30$, $v_{i0} = 0.01$, $T = 0.1$, $U = 1.1$, and $h = 1.2$

Physically, increased ion temperature increases thermal pressure, strengthens the restoring force, and finally yielding sharper, more localized structures. This behaviour is consistent with earlier thermal-effect studies[44,45].

Figure 10 shows how the soliton profile (density) changes with the electron-to-positron density ratio h. It is evident that as h increases, the soliton structure becomes weaker and less localized when the electron population becomes more dominant relative to positrons. This effect is clearly visible in the figure, where the curve corresponding to higher h appears flatter and wider compared to the lower h case. This behaviour can be understood from both the analytical and physical perspectives. Since h directly influences the phase velocity λ_0, an increase in h leads to a reduction in λ_0, From a physical point of view, increasing h introduces a stronger imbalance between electrons and positrons, effectively breaking the symmetry of the plasma. This compositional asymmetry enhances electrostatic screening[9,10] and reduces the efficiency of nonlinear energy localization, making it harder for the system to sustain sharp solitary structures. Together with the earlier results (Figs. 7-9), it becomes clear that dust concentration and compositional imbalance both act to weaken and broaden the soliton. These observations are consistent with recent studies on nonlinear structures in multi-component dusty plasmas[40,43].

Figure 11 illustrates the variation of the electrostatic potential profile with increasing dust change density ($Z_d n_{d0}$). As the dust concentration increases, the potential amplitude decreases while its width increases, following the same trend as the density soliton shown in Fig. 8. Since the electrostatic potential is directly associated with the charge imbalance produced by the density perturbation, any reduction in the density soliton also weakens the corresponding potential pulse. Physically, the presence of negatively charged dust modifies the equilibrium plasma composition and enhances electrostatic screening, thereby reducing the plasma's ability to sustain localized nonlinear structures. This behavior is consistent with earlier theoretical studies on dusty electron-positron-ion plasmas[37,44].

4 Conclusion

The present study of soliton propagation in a homogeneous electron-positron-ion plasma with stationary negatively charged dust reveals that the presence of dust significantly suppresses soliton propagation by reducing wave velocity and soliton amplitude, while increasing soliton width due to enhanced inertia and dispersion. The KdV equation was derived from a multi-fluid plasma model that includes finite-temperature and drift effects, and the solitary wave solution of the KdV equation was analysed for different plasma parameters. On the other hand, ion drift supports wave propagation and partially overcomes the dust-induced reduction of phase velocity. Higher ion temperature enhances the nonlinearity, resulting in taller, narrower solitons. It is observed that dust concentration and compositional imbalance tend to weaken the solitary structures due to stronger electrostatic screening. In summary, the study shows that the balance between nonlinearity and dispersion in dusty pair-plasmas is strongly influenced by the dust concentration, ion drift, thermal effects and plasma composition.

References

1 Zabusky N J & Kruskal M D, *Phys Rev Lett*, 15 (1965) 240.
2 Infeld E & Rowlands G, *Nonlinear waves, solitons and chaos* (Cambridge University Press, Cambridge), 2nd Edn, 2000.
3 Washimi H & Taniuti T, *Phys Rev Lett*, 17 (1966) 996.
4 Sagdeev R Z, *Rev Plasma Phy*, 4 (1966) 23.
5 Davidson R C, *Methods in nonlinear plasma theory*, (Academic Press, New York), 1972 pp. 356.
6 Fried B D & Gould R W, *Phys Fluids*, 4 (1961) 139.
7 Chen F F, *Introduction to plasma physics and controlled fusion* (Springer, Cham), 3rd Edn, 2015 pp. 490.
8 Greaves R G & Surko C M, *Phys Rev Lett*, 75 (1995) 3846.
9 Das A N, Saha S, Raut S & Talukdar P, *Plasma Phys Rep*, 49 (2023) 454.
10 Ruffini R, Vereshchagin G & Xue S S, *Phys Rep*, 487 (2010) 1.
11 Beskin V S, Gurevich A V, Istomin Y N & Arons J, *Physics of the pulsar magnetosphere* (Cambridge University Press, Cambridge), 1993 pp.408.
12 Wardle J F C, Homan D C, Ojha R & Roberts D H, *Nature*, 395 (1998) 457.
13 Greaves R G, Tinkle M D & Surko C M, *Phys Plasmas*, 1 (1994) 1439.
14 Danielson J R, Dubin D H E, Greaves R G & Surko C M, *Rev Mod Phys*, 87 (2015) 247.
15 Iwamoto N, *Phys Rev E*, 47 (1993) 604.
16 Stewart G A & Laing E W, *J Plasma Phys*, 47 (1992) 295.
17 Shukla P K & Stenflo L, *Phys Plasmas*, 13 (2006) 044505.
18 Tajima T & Taniuti T, *Phys Rev A*, 42 (1990) 3587.
19 Gomberoff L, Hoyos J & Muñoz V, *J Geophys Res Space Phys*, 109 (2004) A12107.
20 Kourakis I, Verheest F & Cramer N F, *Phys Plasmas*, 14 (2007) 022306.
21 Zank G P & Greaves R G, *Phys Rev E*, 51 (1995) 6079.
22 Lu G, Ren H, Wu J & Wang Y, *Phys Plasmas*, 12 (2005) 072903.
23 Berezhiani V I & Mahajan S M, *Phys Rev Lett*, 73 (1994) 1110.
24 Shukla P K & Mamun A A, *Introduction to dusty plasma physics* (Institute of Physics Publishing, Bristol), 2002 pp.270.
25 Morfill G E & Ivlev A V, *Rev Mod Phys*, 81 (2009) 1353.
26 Malik H K & Kawata S, *Phys Plasmas*, 14 (2007) 102111.
27 Malik R & Malik H K, *J Theor Appl Phys*, 7 (2013) 65.
28 Salahuddin M, Saleem H & Saddiq M, *Phys Rev E*, 66 (2002) 036407.
29 Shah A & Saeed R, *Phys Plasmas*, 16 (2009) 042304.
30 Mahmood S & Ur-Rehman H, *Phys Plasmas*, 17 (2010) 072305.
31 Esfandyari-Kalejahi A, Saberian E & Akbari-Moghanjoughi M, *Phys Plasmas*, 13 (2006) 122310.
32 Esfandyari-Kalejahi A, Saberian E & Akbari-Moghanjoughi M, *Phys Plasmas*, 13 (2006) 112107.
33 Masood W, Karim S, Shah H A & Siddiq M, *Phys Plasmas*, 16 (2009) 112302.
34 Sabry R, Moslem W M & Shukla P K, *Phys Plasmas*, 16 (2009) 032302.
35 El-Labany S K, Moslem W M & Mowafy A E, *Phys Plasmas*, 18 (2011) 082306.
36 Taniuti T & Wei C C, *J Phys Soc Jpn*, 24 (1968) 941.
37 Malik R, Malik H K & Kaushik S C, *Phys Plasmas*, 19 (2012) 032107.
38 Deepak, Singh D K & Malik H K, Contrib Plasma Phys, (2026) e70161.
39 Malik H K & Malik R, *J Plasma Phys*, 80 (2014) 629.
40 Saini S & Kourakis I, *Phys Plasmas*, 27 (2020) 062109.
41 Saberian E & Esfandyari-Kalejahi A, *Phys Scr*, 86 (2012) 015503.
42 Mamun A A & Jahan N, *Chaos*, 31 (2021) 093135.
43 Hossen M B *et al*., *Astrophys Space Sci*, 367 (2022) 45.
44 El-Labany S K *et al*., *Phys Scr*, 95 (2020) 085601.
45 Bandyopadhyay A & Das K P, *Phys Plasmas*, 30 (2023) 012301.
46 Ghosh B, Banerjee S & Paul S N, *Indian J Pure Appl Phys*, 51 (2013) 488.
47 Gogoi R, Devi N & Das G C, *Indian J Pure Appl Phys*, 46 (2008) 621.
48 Chandra S, *Indian J Pure Appl Phys*, 51 (2013) 715.
49 Malik H K, Singh S & Dahiya R P, *Phys Plasmas*, 1 (1994) 1137.